# Photoelectric Emission from Barium Oxide*

HERBERT R. PHILIPP†
*Department of Physics, University of Missouri, Columbia, Missouri*
(Received April 19, 1957)

Photoelectric emission measurements were made on sprayed coatings of BaO in several states of thermionic activity and at different temperatures. The yield from active cathodes shows a rise at a quantum energy of 3.8 ev ascribed to exciton-induced emission and another rise at 5 ev attributed to electrons ejected from the filled band. A magnetic velocity analyzer was used to determine the energy distribution of emitted electrons. The data indicate that the emission at low quantum energies arises primarily from direct ionization of impurity levels located photoelectrically about 2 ev below the vacuum level. For higher incident quantum energies, where exciton-induced emission is expected, a new energy distribution appears which peaks at very low energy. This peak does not shift with increasing $h\nu$ and is similar to the slow-group distribution observed in the alkali halides.

## INTRODUCTION

In recent years a pointed effort has been made to evaluate the energy level structure of BaO. Careful measurements of photoconductivity and optical absorption of evaporated films and single crystals have established the onset of fundamental absorption at about 3.8 ev and have provided insight into some extrinsic properties of this compound.[1] Photoelectric emission from BaO samples prepared in a variety of ways has determined the energy difference between the top of the valence band and the vacuum level (~5 ev).[2] The present work, while confirming the position of the valence band, is concerned more with processes occurring at lower quantum energies where impurities and imperfections control the photoelectric response. Measurements were made of the spectral distribution of the photoelectric yield and the photoelectron energy distribution. The latter was determined by magnetic analysis. Interpretation of these data is based on established mechanisms for photoelectric emission from $F$ centers in the alkali halides.[3]

## EXPERIMENTAL TECHNIQUES

Two types of vacuum tubes were employed. The first one, a simple diode, was used to measure thermionic and photoelectric emission. The second contained a magnetic velocity analyzer for the measurement of the energy distribution of emitted electrons. A schematic drawing of the analyzer tube is shown in Fig. 1 and a more detailed drawing of the analyzing chamber is shown in Fig. 2. The 3.00-cm-diameter semicircular deflection path is defined by three slits, two $\frac{1}{2}$-mm slits and one $1\frac{1}{2}$-mm slit located just above the cathode position.

The cathode was uniformly sprayed with[4] $BaCO_3$ to a measured weight of approximately 10 mg/cm². The base material was a 0.5-cm² button of spectroscopically pure nickel. After conversion and activation,[5] the tube was sealed off the vacuum system at a pressure of about $10^{-8}$ mm of mercury.

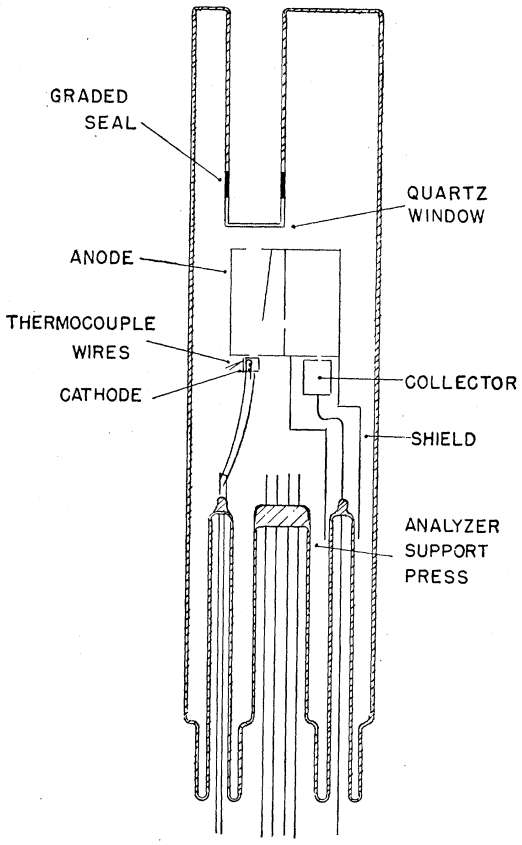


FIG. 1. Schematic drawing of the velocity-analyzer tube. The nickel-molybdenum thermocouple wires are attached to a separate press in the base of the tube not shown in the figure.

* Supported in part by the Office of Naval Research.
† Now at the General Electric Research Laboratory, Schenectady, New York.
[1] E. O. Kane, J. Appl. Phys. **22**, 1214 (1951); W. W. Tyler and R. L. Sproull, Phys. Rev. **83**, 548 (1951); W. C. Dash, Phys. Rev. **92**, 61 (1953); R. J. Zollweg, Phys. Rev. **97**, 288 (1955).
[2] Apker, Taft, and Dickey, Phys. Rev. **84**, 508 (1951).
[3] L. Apker and E. Taft, Phys. Rev. **79**, 964 (1950); **81**, 698 (1951); **82**, 814 (1951).
[4] Ultra-pure $BaCO_3$ was obtained from Mallinckrodt Chemical Works.
[5] G. Hermann and S. Wagener, *The Oxide-Coated Cathode* (Chapman and Hall, Ltd., London, 1951), Vol. 1.

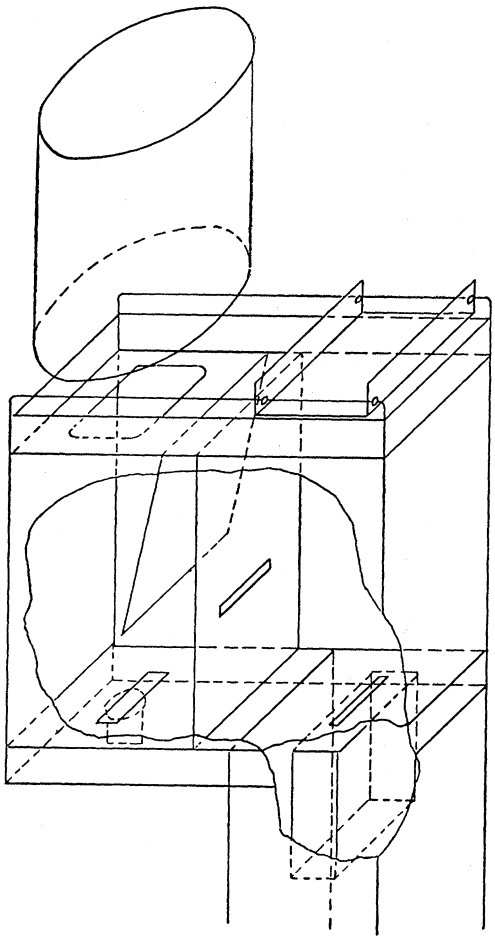

FIG. 2. Detailed drawing of the analyzing chamber. The 3.00-cm-diameter semicircular deflection path is defined by three slits, two ½-mm slits and one 1½-mm slit located just above the cathode position. A sliding cover could be placed over the upper light port to protect the quartz window from evaporation products during conversion and activation of the sample.

A 1000-watt type AH6 high-pressure mercury arc, in conjunction with a Gaertner monochromator, served as a continuous source of high-intensity radiation throughout the spectral region extending down to about 2600 A. Low-pressure mercury and zinc arcs were employed for measurements in the far ultraviolet.

## PROCEDURES FOR MEASURING ENERGY DISTRIBUTIONS

Electrons emitted from the cathode were accelerated to the anode by a positive voltage large enough to produce saturation emission. This voltage was kept relatively small, between 5 and 10 volts, so as to make it unnecessary to use large magnetic fields. The collector potential was the same as at the anode.

The magnetic-field requirements can be calculated from the expression

$$V=\tfrac{1}{2}(e/m)H^2R^2, \qquad (1)$$

where $R$ is the radius of the semicircular deflection path, $H$ is the magnetic field, and $V$ is the energy of the electrons passing through the slit system. Evaluating the constants and setting $R=1.50$ cm, this becomes

$$V=0.198H^2, \qquad (2)$$

where $H$ is in gauss and $V$ in volts.

A pair of Helmholtz coils served as a source of uniform magnetic field. For the 36.4-cm radius coils, the expression for the energy of the electrons reaching the collector in terms of the coil current $I$ in amperes is

$$V=0.984I^2. \qquad (3)$$

The coils were connected in series and the current was measured by observing the voltage across a standard 0.01-ohm resistor placed in the circuit.

The thermionic properties of the cathode were used to calibrate the analyzer and to determine the zero of energy point for photoelectric distributions. The number of thermionic electrons escaping unit area per unit time with energy between $E$ and $E+dE$ is given by[6]

$$g(E)dE=n(2\pi m)^{-\frac{1}{2}}(kT)^{-\frac{3}{2}}Ee^{-E/kT}dE. \qquad (4)$$

The peak of this distribution occurs at $E_p=kT$. A

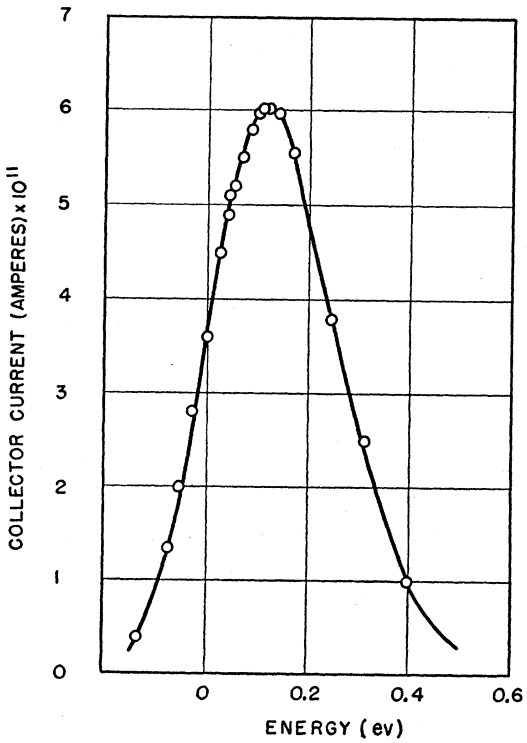


FIG. 3. Typical energy distribution of emitted thermionic electrons for a cathode temperature of 740°K. The collector current at the peak of this distribution is about one-hundredth of the anode current ($6\times10^{-9}$ ampere).

[6] I. L. Sparks and H. R. Philipp, J. Appl. Phys. 24, 453 (1953).

typical experimental thermionic energy distribution curve is shown in Fig. 3.[7]

The analyzer was calibrated by plotting the square of the Helmholtz-coil current at the peak of the thermionic distribution *vs* anode voltage with the cathode at a fixed temperature. This plot, shown in Fig. 4, was a straight line after a correction was made for the effect of the earth's magnetic field.[8] The slope of this graph, 0.986, may be compared to the calculated value of 0.984 in Eq. (3). The zero-current intercept on the voltage axis is the contact potential between the cathode and the clean tantalum anode.

For photoelectric distributions, the anode voltage was set at some arbitrary value, usually 8.0 volts. The linearity of the calibration curve made it unnecessary to know the voltage setting to any great degree of accuracy, although once fixed it must remain at this value during a run. The zero of energy was determined from concurrent thermionic distributions.[9] The area of each distribution was determined by graphical integration and equated to the yield at the same value of incident quantum energy. This converts the collector-current scale to absolute units, electrons per quantum per ev.

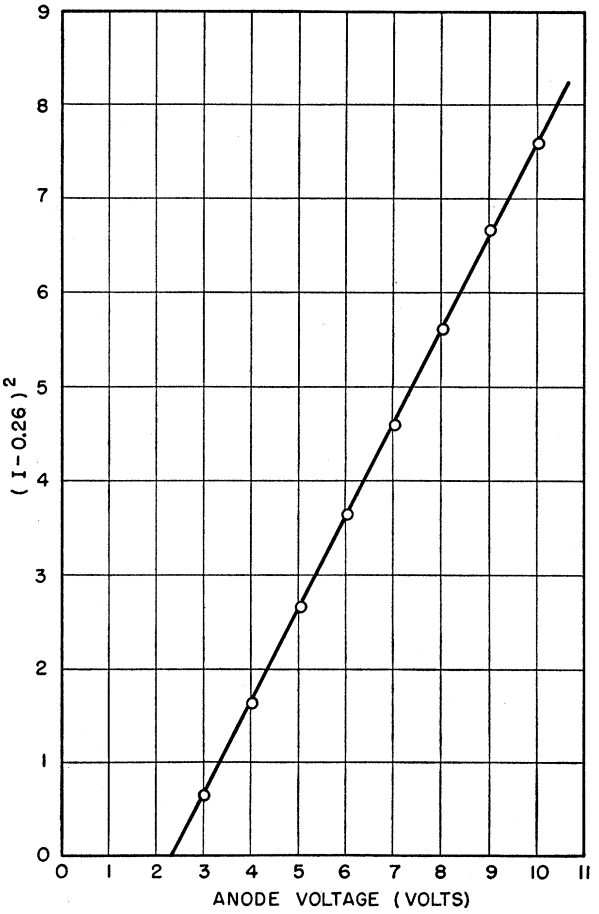


FIG. 4. Calibration of the velocity analyzer. A Helmholtz-coil current, $I$, of 0.26 ampere is required to nullify the oppositely directed magnetic field of the earth (see reference 8). The intercept on the voltage axis is the anode-cathode contact potential.

## EXPERIMENTAL RESULTS

The effect of light striking the cathode is to produce a photoelectric emission and an enhancement of this emission.[10] These effects are particularly prominent in in the region of fundamental absorption.[11] Irradiation at 3.8 ev may increase the emission at longer wavelengths by more than a factor of 100. These processes were studied and found to depend on a number of variables including (1) the wavelength of the enhancing light, (2) the wavelength at which the effect is observed,

[7] Because of the finite resolution of the analyzer, it is expected that some of the points should fall at "negative energies." The analyzer was designed for the measurement of low-current photoelectric distributions. The observed thermionic distribution, $G(E,T)$, can be written as $G(E,T)=\int_{\Delta=-E}^{\infty} w(\Delta)g(E+\Delta, T)d\Delta$, where $w(\Delta)$ is the slit function, and $g(E,T)$, the theoretical distribution, is given by Eq. (4). In a simple case, the slit may be assumed to pass electrons with unit probability in the energy range $D$. Thus $dw/d\Delta=[\delta(\Delta+D/2)-\delta(\Delta-D/2)]$ and $dG/dE=g(E-D/2, T)-g(E+D/2, T)$. To determine the position of the peak, we set this equal to zero and find $E_p=(D/2)\coth(D/2kT)$. For small $D$, of course, this is $kT$, but as $D$ increases the position of the maximum moves toward higher energy and the shift with temperature decrease to some value less than $k$. It was found that the shape of thermionic energy distributions at different temperatures could be accurately fitted by using a slightly more comlicated slit function having a primary half-width of 0.1 ev.

[8] The tube was placed in a north-south direction for use with the magnetic field vertical. A compressed-air driven magnetic null indicator, positioned at the analyzing-chamber location, indicated the net vertical field was zero with 0.26 ampere flowing through the Helmholtz coils. This value may be converted to give the vertical component of the earth's magnetic field, 0.58 gauss (inclination of 70°).

[9] The temperature dependence of the contact potential was measured by observing these distributions at different cathode temperatures. It was found that the peak of the thermionic distribution shifted slightly as the temperature of the cathode was changed. The shift was larger than the factor $k\Delta T$ and was ascribed to the temperature dependence of the work function which alters the anode-cathode contact potential. A straight line was obtained when the energy at the peak of each distribution was plotted as a function of temperature, yielding a value for the temperature dependence of the work function. This value was compared to that obtained from an interpretation of the experimental Richardson plot. The slope of this plot is a measure of the Richardson work function, $\phi_R$, where $\phi_R=\phi+T(d\phi/dT)$. Thus the equation $A^*e^{(e/k)(d\phi/dT)}=A_0=120$ amp/cm² °K² relates the experimental $A$ constant, $A^*$, and the theoretical value to the temperature dependence of the work function. This comparison, for three cathodes, is shown in the table below.

| $\phi_R$ (ev) | $A^*$ (amp/cm² °K²) | $J_{1000°K}$ (amp/cm²) | $\phi_{1000°K}$ (ev) | $d\phi/dT$ from $A$ constant (ev/°K) | $d\phi/dT$ from distributions (ev/°K) |
|---|---|---|---|---|---|
| 1.8 | 0.53 | $3.3\times10^{-4}$ | 2.3 | $4.7\times10^{-4}$ | $5.3\times10^{-4}$ |
| 2.1 | 3.07 | $6.0\times10^{-5}$ | 2.4 | $3.2\times10^{-4}$ | $2.8\times10^{-4}$ |
| 2.8 | 760 | $4.5\times10^{-6}$ | 2.6 | $-1.6\times10^{-4}$ | $-2.3\times10^{-4}$ |

The agreement is surprisingly good. In obtaining the zero of energy for the photoelectric distributions, the temperature dependence of the contact potential was taken into consideration. For further discussion see C. Herring and M. Nichols, Revs. Modern Phys. **21**, 185 (1949); G. Hermann and S. Wagener, reference 5, Vol. 2, p. 191.

[10] B. D. McNary, Phys. Rev. **81**, 631 (1951).

[11] J. E. Dickey and E. A. Taft, Phys. Rev. **80**, 308 (1950).

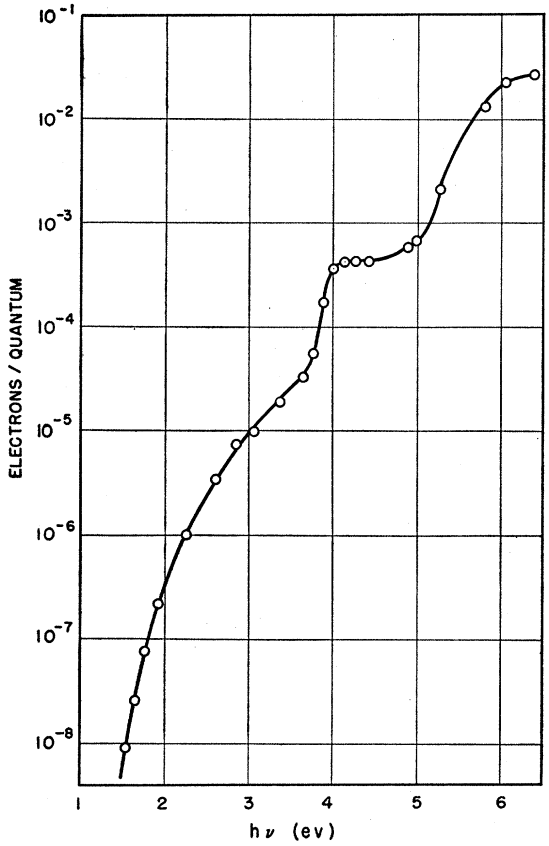


FIG. 5. Spectral distribution of the photoelectric yield for BaO extended to quantum energies above 5 ev.

(3) the intensity of the enhancing light, (4) the temperature of the cathode, (5) the state of thermionic activity of the cathode, and (6) the past irradiation history of the cathode.

In the data presented below, these time-dependent effects were kept to a minimum. Measurements were made as quickly as possible starting with the longer wavelengths which are least effective in altering the cathode emission. The cathode was also heated at convenient intervals to reduce the effects of past irradiation.

## SPECTRAL DISTRIBUTION OF THE PHOTOELECTRIC YIELD

The spectral distribution of the photoelectric yield for a BaO sample is shown in Fig. 5. The curve exhibits a rise in yield at 3.8 ev and a larger increase in yield for quantum energies above 5 ev.

Data were generally confined to the spectral region of the *AH6* arc and compared to concurrent thermionic-emission data. The yield curve for a cathode having a Richardson work function of 1.8 ev and a zero-field thermionic emission at 1000°K of $3\times10^{-4}$ amp/cm² is shown in Fig. 6 (curve *a*). This sample was then deactivated by exposure to oxygen at an elevated temperature. The zero-field thermionic emission at 1000°K decreased by about two decades. This curve is also shown in Fig. 6 (curve *b*). The yield is about a factor of two less in the region above 3.5 ev but then drops off rapidly at lower quantum energies. The cathode was deactivated a second time to a thermionic level of $1\times10^{-8}$ amp/cm² at 1000°K and a Richardson work function of 2.8 ev. The curve for this state of activation is shown in Fig. 7. The response differs in several aspects from the previous data. A decrease in emission is observed in the region of 3.8 ev and no detectable yield is found below 2.2 ev.

Samples were investigated having thermionic work functions as high as 3.4 ev. Here the threshold of observable photoemission was above 4 ev. In cathodes showing emission at 2 ev, the rise in yield at 3.8 ev was also observed. For incident quantum energies above 4.8 ev, the yield from all samples approached the same value.

## TEMPERATURE DEPENDENCE OF THE PHOTOELECTRIC YIELD

For quantum energies below 2 ev, the photoelectric yield increased with increasing temperature, the larger

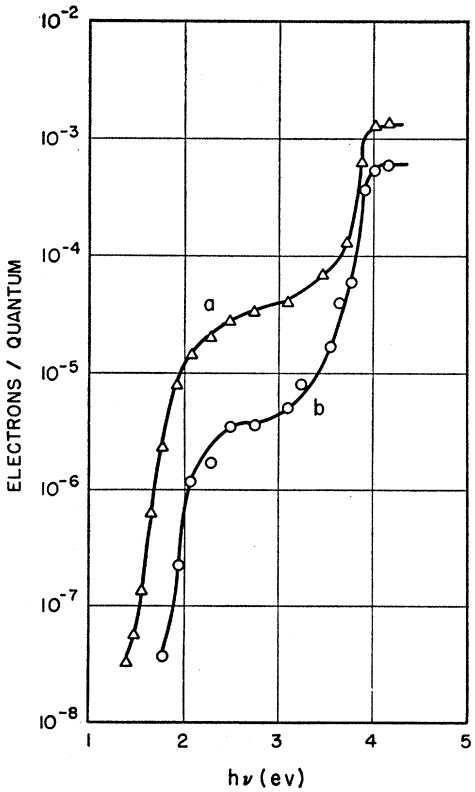


FIG. 6. Spectral distribution of the photoelectric yield for a BaO sample in several states of thermionic activity. A cathode having a Richardson work function of 1.8 ev and a zero-field thermionic emission at 1000°K of $3\times10^{-4}$ amp/cm² (curve *a*) was deactivated to a thermionic state having a Richardson work function of 2.6 ev and a zero-field thermionic emission at 1000°K of $3\times10^{-6}$ amp/cm² (curve *b*).

relative increase being at the longer wavelengths. Measurements made on an active cathode are shown in Fig. 8. The emission at 1.38 ev has increased by more than a factor of ten for the approximately 200°K increase in temperature. No temperature dependence was observed in the region between 2 and 3 ev. Above about 3.2 ev, the emission decreased with increasing temperature. The observed dependence for a quantum energy of 4.14 ev is shown in Fig. 9. Here the logarithm of the emission is plotted as function of $1/T$. The slope is equivalent to an activation energy of 0.15 ev.

## ENERGY DISTRIBUTIONS

The energy distribution of emitted photoelectrons for a cathode having a Richardson work function of 2.1 ev and an emission at 1000°K of $6\times10^{-5}$ amp/cm² is shown in Fig. 10 for five values of incident quantum energy. The yield curve for this sample is similar to that shown in Fig. 5. Two types of distributions are observable. One, which moves linearly toward higher energy with increasing $h\nu$, is termed the $f$ group ($f$ for fast). The difference in energy between the incident quantum value and the escape energy at the peak of the $f$ group is constant and equal to about 2 ev. The second, termed the $s$ group ($s$ for slow), appears at very low energy and does not shift with increasing quantum energy. For low values of incident quantum energy only the $f$ group is seen and it appears quite symmetrical in shape. At 3.54 ev, this distribution shows some added structure on the low-energy side of the curve. The $s$ group is fully developed at 4.13 ev.

The energy distribution of emitted photoelectrons for a sample in a higher state of thermionic activity is shown in Fig. 11. These curves are plotted on a logarithmic scale which avoids the use of multiplying

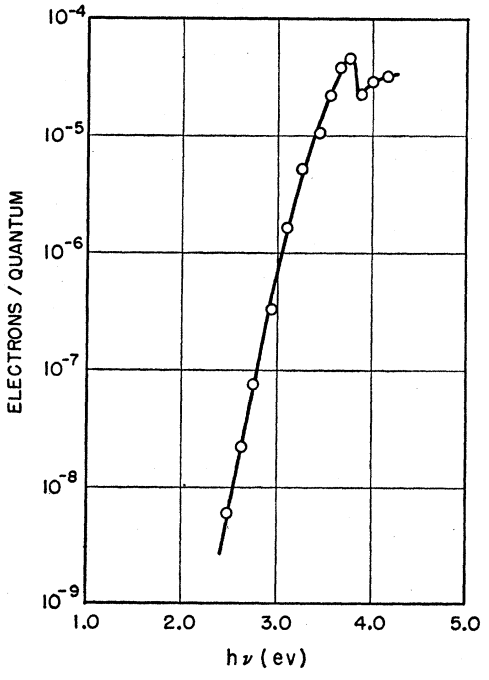


FIG. 7. Spectral distribution of the photoelectric yield for a BaO sample having a Richardson work function of 2.8 ev and a zero-field thermionic emission at 1000°K of $1\times10^{-8}$ amp/cm². Photoelectric data for this cathode in higher states of thermionic activity are shown in Fig. 6.

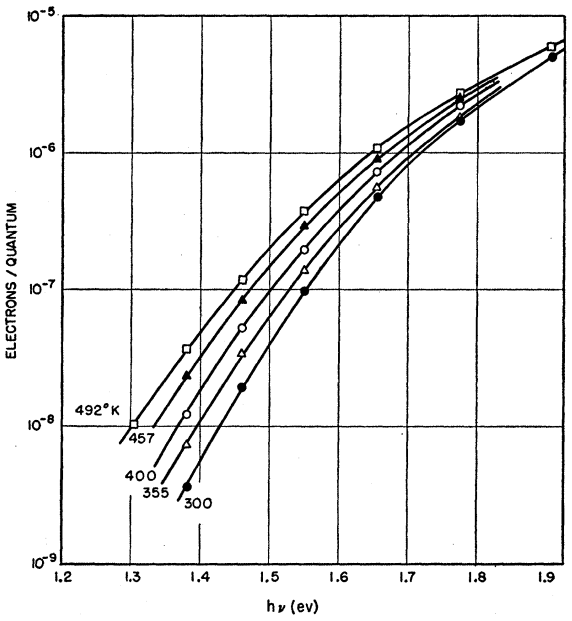


FIG. 8. Spectral distribution of the photoelectric yield, at low quantum energies, for a BaO sample at five different temperatures.

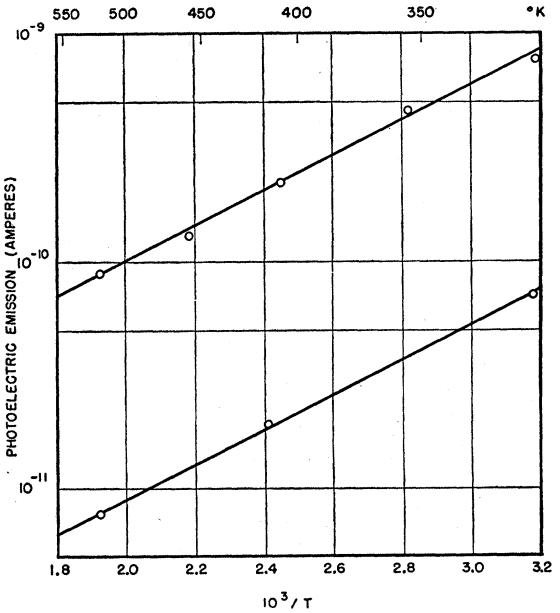


FIG. 9. Temperature dependence of the photoelectric emission from BaO for an incident quantum energy of 4.14 ev. The light intensity is about a factor of ten greater for the upper curve.

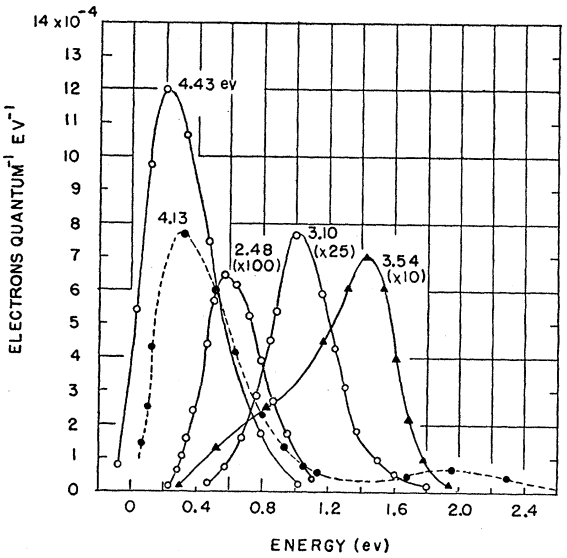


FIG. 10. Energy distribution of the photoelectric yield from BaO for 5 values of incident quantum energy. The yield curve for this sample is similar to that shown in Fig. 5. The ordinates of several of these curves have been multiplied by the scale factors indicated.

factors and helps show interesting features not seen in the previous curves. The yield curve for this cathode is shown in Fig. 6 (curve *a*).

The *f* group is symmetrical for low values of incident quantum energy. As the energy is increased, the *f* group broadens and at 2.95 ev the distribution shows added structure on the low-energy side. This probably marks the appearance of the *s* group which, for higher quantum energies, increases in size while the *f* group peak height remains about the same. The *s* group predominates at 3.88 ev.

The effect of increasing the temperature is to broaden the *f* group and to decrease the height of the *s* group. Irradiating the cathode in the region of fundamental absorption shifts the peaks of the *f* and *s* groups to slightly lower energy. This shift, associated with enhanced photoelectric emission, results from small changes in the anode-cathode contact potential.

Some data were obtained on a deactivated sample, the yield curve for which is shown in Fig. 7. For an incident quantum energy of 3.45 ev, the energy distribution was symmetrical with a peak at about 0.4 ev. For higher quantum energies, above 3.8 ev, the curves showed added structure. Collector currents were extremely small here and the precision of the data does not merit a more exact description. It may be said, however, that the distributions differ in gross detail from those obtained on cathodes showing emission at 2 ev and a rise in yield at 3.8 ev. No *f* group is found nor any distribution which may be associated with the *s* group of more active samples.

## DISCUSSION AND CONCLUSIONS

The origin of the photoelectric emission from BaO may be divided into two parts. Above 5 ev, the rise in yield is attributed to electrons ejected from the filled band and is an intrinsic property of the pure crystal. The onset of this process is a measure of the energy difference between the top of the filled band and the vacuum level. The variable yield at lower quantum energies is ascribed to electronic levels located in the forbidden band and associated with impurities and imperfections in the BaO lattice.[12]

The results of this paper are mainly concerned with emission from centers associated with impurities and imperfections. For incident quantum energies below 3 ev, the symmetrical energy distribution of the *f* group indicates that the emission arises from direct photoionization of impurity electrons centered at a photoelectric energy depth of 2 ev below the vacuum level. An energy-level diagram for this type of emission, devised by Herring,[13] is discussed by Apker and Taft in describing the photoelectric emission from *F* centers in RbI.[14]

The wings of this distribution should broaden as the temperature is increased, the various configurations assumed by the center having a Boltzmann distribution in energy. The most sensitive method of observing this is shown in Fig. 8. At 1.4 ev, where the emission is only from the wing of the 2-ev distribution, the yield increased with temperature. At 2 ev, the constant yield between 300 and 500°K indicates a constant number of electrons available for this emission. This temperature dependence is consistent with the Herring model.

For incident quantum energies above 3 ev, the distributions show that a new emission process is competing with direct ionization. This is illustrated by the appearance of the *s* group. As the energy is further increased, more and more of the additional electrons appear in the *s* group, the *f* group remaining approximately constant in area. At 3.88 ev, almost all the yield is associated with the *s* group.

The mechanism of photoelectric emission in the *s* group, in apparent contrast to the simpler process of direct ionization, has been ascribed to a two-step process. The incident quanta produce excitons which transfer energy to impurity electrons and thus cause the release of these electrons to the vacuum. The greater efficiency of exciton-induced emission (high absorption) explains the rise in yield, but additional theory is required if the shape of the energy distribution is to be described.[15]

Some expected qualitative features of the exciton-induced emission can be confirmed in each phase of this two-step process. Increasing the temperature should increase the probability that excitons are thermally

[12] This interpretation was first presented by Apker, Taft, and Dickey, reference 2.
[13] C. Herring, Phys. Rev. **73**, 1238T (1948).
[14] L. Apker and E. Taft, Phys. Rev. **82**, 814 (1951).
[15] F. Seitz, Revs. Modern Phys. **26**, 7 (1954).

dissociated before energy transfer to impurity sites. At higher temperatures the exciton-induced yield decreases. An activation energy of 0.15 ev for this process suggests that the band gap of BaO is close to 4 ev.

The second step of the exciton-induced emission process is the ejection of electrons from stimulated impurity centers. If these levels were empty, production of excitons would still take place although no external emission would be observable. The exciton would either recombine or thermally dissociate. The exciton-induced rise in the yield was only observed when there was also a detectable emission in the region of 2 ev. Energy distributions obtained from a sample having no measurable yield at 2 ev did not show an *s*-group distribution. The yield curve for this sample shows a decrease in emission at 3.8 ev.[16] Thus, the centers responsible for the induced external photoelectrons appear to lie only in the 2-ev level. Deeper lying levels may also be exciton stimulated but not enough energy is given these electrons for them to cross the potential barrier at the crystal surface.

It should be pointed out that the energy distributions for the more active cathode show the appearance of the *s* group for quantum energies as low as 2.95 ev. The energy required for exciton production at dislocations, grain boundaries, surfaces, impurity centers, etc., may be less than that required for production in the bulk, 3.8 ev.[17]

Detail corresponding to the multiplet exciton absorption in BaO should be observed in the photoelectric yield.[18] Some structure was found, particularly in samples of low thermionic activity, however the precision of these data does not compare with that obtainable in optical-transmission studies. It would be of great interest to use lower sample temperatures to determine whether or not this structure becomes pronounced.

The photoelectric effects in BaO show a surprising correspondence to processes in the alkali halides and interpretations used for these salts have been freely applied to similar observations in BaO. Energy distribution curves are practically identical in character. The ability of the BaO cathode to emit thermionic electrons when heated has been associated with donor levels located relatively near the conduction band. These permanent centers, possibly electrons in vacancies, may be likened to *F* centers in the alkali halides.

In the alkali halides, the concentration of *F* centers near the crystal surface is so high ($>10^{18}$ cm$^{-3}$) as to make it impossible to distinguish between energy-transfer processes in the exciton-induced photoelectric yield.[19] In BaO, the density of these centers, as measured by the yield at 2 ev (or perhaps in a more complicated way by the thermionic emission), may be varied over a considerable range. The yield at 3.8 ev, however, is relatively constant. This is consistent with exciton migration, but absolute values for the density of these centers are needed before a cross section for exciton-induced emission can be calculated.

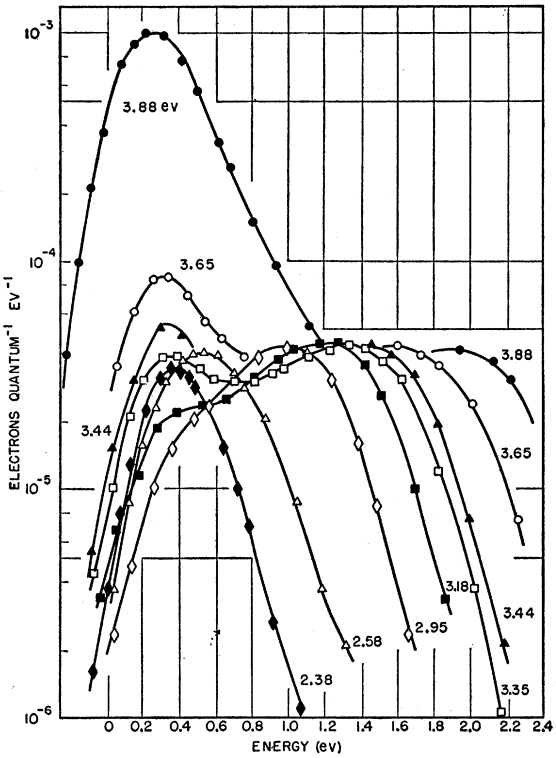


FIG. 11. Energy distribution of the photoelectric yield from BaO for 8 values of incident quantum energy. The yield curve for this sample is shown in Fig. 6 (curve *a*).

## ACKNOWLEDGMENTS

The author wishes to express his deep appreciation to the late Professor Albert S. Eisenstein under whose guidance this investigation was carried through its formative stages and to Professor Eugene B. Hensley and Professor Bernard Goodman for many stimulating conversations. The author is also indebted to Dr. L. Apker for his critical review of this manuscript and to the Minneapolis Honeywell Regulator Company and the Office of Naval Research for financial assistance during this period.

[16] This type of yield curve was observed by H. B. DeVore and J. W. Dewdney, Phys. Rev. **83**, 805 (1951), in unactivated BaO samples.

[17] E. Taft and L. Apker, J. Chem. Phys. **20**, 1648 (1952).

[18] R. J. Zollweg, Phys. Rev. **97**, 288 (1955); A. W. Overhauser, Phys. Rev. **101**, 1702 (1956).

[19] H. R. Philipp and E. A. Taft, Phys. Rev. **106**, 671 (1957).